Experimental confirmation of spin gap in antiferromagnetic alternating spin-$\frac{3}{2}$ chain substances RCrGeO$_5$ (R=Y or ^{154}Sm) by inelastic neutron scattering experiments

Masashi Hase,[1,*] Minoru Soda,[2] Takatsugu Masuda,[2] Daichi Kawana,[2,3] Tetsuya Yokoo,[3] Shinichi Itoh,[3] Akira Matsuo,[2] Koichi Kindo,[2] and Masanori Kohno[1]

[1]*National Institute for Materials Science (NIMS), Tsukuba, Ibaraki 305-0047, Japan*

[2]*The Institute for Solid State Physics (ISSP), the University of Tokyo, Kashiwa, Chiba 277-8581, Japan*

[3]*High Energy Accelerator Research Organization (KEK), Tsukuba, Ibaraki 305-0801, Japan*

(Received 28 February 2014; revised manuscript received 7 July 2014; published 21 July 2014)

A spin-singlet ground state with a spin gap has been discovered in antiferromagnetic spin chain substances when the spin value is 1/2, 1, or 2. To find spin-gap (singlet-triplet) excitations in spin-$\frac{3}{2}$ chain substances, we performed inelastic neutron scattering and magnetization measurements on RCrGeO$_5$ (R = Y or Sm) powders. As expected, we observed spin-gap excitations and the dispersion relation of the lowest magnetic excitations. We proved that the spin system of Cr^{3+} was an antiferromagnetic alternating spin-$\frac{3}{2}$ chain. We describe the influence of frustration between nearest-neighbor and next-nearest-neighbor exchange interactions in the chain.

DOI: 10.1103/PhysRevB.90.024416 PACS number(s): 75.10.Pq, 75.10.Kt, 75.40.Gb

I. INTRODUCTION

The ground state (GS) is spin singlet in antiferromagnetic (AF) Heisenberg alternating spin chains because of large quantum fluctuation. The Hamiltonian is given as follows:

$$\mathcal{H} = J \sum_i [1 - (-1)^i \delta] \boldsymbol{S}_i \cdot \boldsymbol{S}_{i+1}. \quad (1)$$

In the AF Heisenberg uniform ($\delta = 0$) spin-$\frac{1}{2}$ chain, GS is almost an ordered state in spite of spin singlet (critical state) and is designated the gapless Tomonaga-Luttinger liquid (TLL). A gapless GS can also appear when the spin value S is larger than 1/2 [1–4]. The gapless GS is regarded as TLL. A spin gap (singlet-triplet gap) opens except for gapless point(s) and a spin-singlet GS is stabilized. The spin-singlet GS can be expressed using valence-bond-solid (VBS) diagrams, as depicted in Fig. 1 [3]. Considering the range of δ in which VBS exists, the appearance of the spin gap is a common phenomenon in AF alternating spin chains.

Model substances have been found for the hatched GSs in Fig. 1 when $S = 1/2, 1$, and 2. $Cu(NO_3)_2$-$2.5H_2O$ [5,6], TTF-$MS_4C_4(CF_3)_4$ (M = Cu or Au, TTF = tetrathiafulvalene) [7,8], and $CuGeO_3$ [9–11] are model substances for $S = 1/2$ (a). [Ni(N,N'-bis(3-aminopropyl)propane-1, 3-diamine(μ-NO_2)]ClO_4 (abbreviated as NTENP) [12,13] is a model substance for $S = 1$ (a). $Ni(C_2H_8N_2)_2NO_2(ClO_4)$ (abbreviated as NENP) [14] and Y_2BaNiO_5 [15–17] are model substances for $S = 1$ (c).

When the spin value is larger than 1, almost no model substance showing a spin gap exists. The only example reported in the literature is $MnCl_3(C_{10}H_8N_2)$ [18]. This substance has an AF uniform spin-2 chain of which GS is shown by the diagram of $S = 2$ (c). The energy gap was evaluated as 0.32(8) and 0.14(3) meV from magnetization curves at 30 mK in the magnetic field parallel and perpendicular to chains, respectively. These gaps are consistent with a Haldane gap of 0.20(7) meV, where the excited triplet is split by single-ion anisotropy $D = 0.03(1)$ meV. The temperature T dependence of magnetic susceptibility and the magnetization curve were well fitted to calculated results with $J = 31.2$ K and the g value of 2.02 [19]. Inelastic neutron scattering results provide microscopic evidence for the presence of the Haldane gap [20]. $Cr_2[BP_3O_{12}]$ has AF alternating spin-$\frac{3}{2}$ chains [21]. The substance shows a magnetic order below 28 K. The existence of a spin gap was not investigated. The value of δ was evaluated as 0.33 that is close to the gapless point [0.42(2)]. A presumable small spin gap and interchain interactions cause the magnetic order.

We comment on AF Heisenberg uniform spin chain substances AMX_3. Here A is K, Rb, or Cs; M is a 3d atom; and X is F, Cl, or Br. In the uniform spin-1 chain substance $CsNiCl_3$, the Haldane gap was observed in inelastic neutron scattering experiments [22]. In the uniform spin-$\frac{3}{2}$ chain substances $CsVCl_3$ and $CsVBr_3$, low-energy broad excitations were observed at the magnetic zone center at 20 K ($>T_N = 13.3$ K) [23] and 25 K ($>T_N = 20.3$ K) [24], respectively, where T_N is an AF transition temperature. The low-energy broad excitations were recognized as a part of the continuum just above the lowest magnetic excitations. Therefore, the experimental results do not contradict the theoretical prediction (gapless excitations). In the uniform spin-2 chain substance $CsCrCl_3$, no excitation gap was detected at the magnetic zone center at 20 K ($>T_N =$ 16 K) within the experimental errors [25]. The Haldane gap can be estimated to be 0.2 meV and is predicted to be observable below 1.4 K. Thus, the Haldane gap was unable to be detected in the experiments.

We can show experimentally that the appearance of the spin gap is a universal phenomenon irrespective of the spin value below 2 if we can find the spin gap in an AF alternating spin-$\frac{3}{2}$ chain substance. We have devoted attention to insulating RCrGeO$_5$ (R = Y or rare earth) as shown in Fig. 2 [26]. A Cr^{3+} ion is surrounded by O^{2-} ligands and forms a CrO_6 octahedron. In the GS of Cr^{3+} ions, the orbital degree of freedom is quenched. Spin-$\frac{3}{2}$ is responsible for the magnetism of Cr^{3+} ions. From the crystal structure, Cr^{3+} spins are expected to form an alternating spin-$\frac{3}{2}$ chain. Table I shows

*HASE.Masashi@nims.go.jp

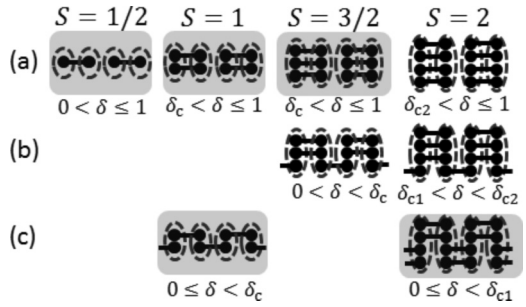

FIG. 1. The valence-bond-solid (VBS) diagrams [3]. The spin-singlet GSs shown in (a), (b), and (c) is designated $(2S,0)$, $(2S-1,1)$, and (S,S) states, respectively. Small circles and lines represent spin-$\frac{1}{2}$ variables and singlet pairs, respectively. Each ellipse represents the symmetrization of the spin-$\frac{1}{2}$ variables on each site to create the total spin variable. The GSs are accompanied with a spin gap. The value of δ of gapless points is 0 for $S = 1/2$, $\delta_c = 0.2595(5)$ for $S = 1$ [2], 0 and $\delta_c = 0.42(2)$ for $S = 3/2$ [3], and $\delta_{c1} = 0.18(1)$ and $\delta_{c2} = 0.545(5)$ for $S = 2$ [4]. Model substances were found for the hatched GSs when $S = 1/2, 1$, and 2, as described in the text. In this study, we show that RCrGeO$_5$ (R = Y or Sm) are model substances for the hatched GS of $S = 3/2$ (a).

the Cr-O-Cr angle and Cr-Cr distance in two kinds of Cr-Cr bonds (d_1 and d_2 bonds). Spin chains are separated from one another by GeO$_5$ square pyramids and R^{3+} ions. Shpanchenko *et al.* reported the T dependence of magnetic susceptibility (χ) of RCrGeO$_5$ (R = Sm, Eu, or Nd) powders [26]. A broad maximum of χ appears at $T_{max} = 220$ K and 100 K in SmCrGeO$_5$ and EuCrGeO$_5$, respectively, indicating the existence of a low-dimensional AF spin system. Considering the crystal structure and the large values of T_{max}, we can expect that Cr^{3+} spins form an AF Heisenberg alternating spin-$\frac{3}{2}$ chain. No magnetic transition appears down to 1.8 K in the two substances. In NdCrGeO$_5$, χ of Nd^{3+} ions is very large. We cannot determine whether χ of Cr^{3+} spins shows a broad maximum or not. Probably, an AF alternating spin-$\frac{3}{2}$ chain also exists in NdCrGeO$_5$ because of the same crystal structure. A clear peak appears at 2.6 K in χ of NdCrGeO$_5$. The susceptibility of Nd^{3+} ions is dominant at low T. Probably, Nd^{3+} magnetic moments generate a magnetic transition.

As T is lowered, the susceptibility of RCrGeO$_5$ (R = Sm, Eu, or Nd) increases like a Curie-Weiss susceptibility. The increase originates in rare-earth ions or magnetic other

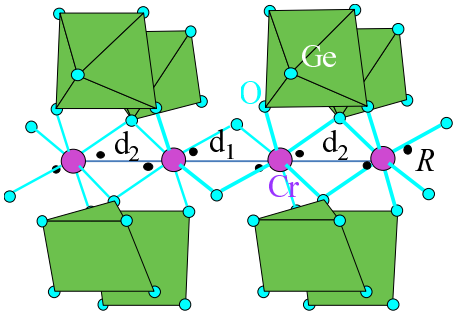

FIG. 2. (Color online) A part of the RCrGeO$_5$ structure showing two kinds of Cr-Cr bonds in the chain of edge-sharing CrO$_6$ octahedra, GeO$_5$ square pyramids, and R atoms.

TABLE I. Cr-O-Cr angles and Cr-Cr distances in two kinds of Cr-Cr bonds (d_1 and d_2 bonds) in RCrGeO$_5$ (R = Y or Sm) [26].

		Y	Sm
d_1 bond	Cr-O-Cr angle	95.9°	97.3°
	Cr-Cr distance	2.872 Å	2.952 Å
d_2 bond	Cr-O-Cr angle	92.8°	91.3°
	Cr-Cr distance	2.811 Å	2.770 Å

materials. The susceptibility becomes nearly zero at low T if a spin-singlet GS with a spin gap exists in the Cr^{3+} spin system. Because of the Curie-Weiss susceptibility at low T, unfortunately, we cannot prove a spin-singlet GS with a spin gap from the susceptibility results. Consequently, we performed inelastic neutron scattering (INS) and magnetization measurements on RCrGeO$_5$ (R = Y or Sm) powders to confirm the spin-gap (singlet-triplet) excitations.

II. METHODS OF EXPERIMENTS AND CALCULATIONS

Crystalline powders of RCrGeO$_5$ (R = Y or Sm) were synthesized using a solid-state-reaction method at 1523 K in air with intermediate grindings [26]. We used an isotope ^{154}Sm (purity of the isotope, 99%) for powders of INS experiments to decrease absorption of neutrons. We confirmed formation of RCrGeO$_5$ (R = Y or Sm) using an x-ray diffractometer (RINT-TTR III; Rigaku). We were able to obtain samples of a nearly single phase of SmCrGeO$_5$. We found the existence of nonmagnetic $Y_2Ge_2O_7$ in diffraction patterns of YCrGeO$_5$ samples. The molar ratio of $Y_2Ge_2O_7$ was estimated roughly as 10% from diffraction intensities.

We measured magnetizations up to $H = 5$ T using a superconducting quantum interference device (SQUID) magnetometer (MPMS-5S; Quantum Design). High-field magnetization measurements were conducted using an induction method with a multilayer pulsed field magnet installed at the Institute for Solid State Physics, the University of Tokyo. We performed INS measurements using the High Resolution Chopper spectrometer at BL 12 in the Japan Proton Accelerator Research Complex (J-PARC) [27–29]. The energy resolution at the energy transfer $\omega = 0$ meV is 3%–5% of E_i (the energy of incident neutrons). The Q resolution is better than 0.1 Å^{-1}, where Q is the magnitude of the scattering vector.

We calculated susceptibility of AF Heisenberg alternating spin-$\frac{3}{2}$ chains [Eq. (1)] using the quantum Monte Carlo loop algorithm [30] on 240 site chains. Finite-size effects and statistical errors are negligible in the scales of figures represented in this paper. We calculated the dynamical structure factor, which is proportional to neutron scattering intensity, on 120 site chains under the open boundary condition using the dynamical density-matrix renormalization group (DMRG) method [31].

III. RESULTS AND DISCUSSION

We show χ of YCrGeO$_5$ and SmCrGeO$_5$ powders as red circles in Figs. 3(a) and 3(b), respectively. The value of the applied magnetic field is 0.01 T. The molar ratio of $Y_2Ge_2O_7$ included in the YCrGeO$_5$ sample was estimated

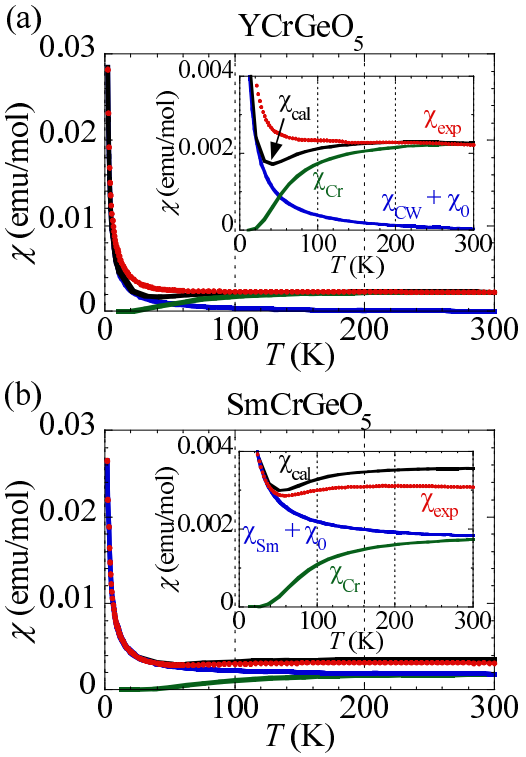

FIG. 3. (Color online) Magnetic susceptibility in 0.01 T of $YCrGeO_5$ (a) and $SmCrGeO_5$ (b). The insets represent χ below 0.004 emu/mol. Circles show the experimental results. Three lines in each figure are explained in the text.

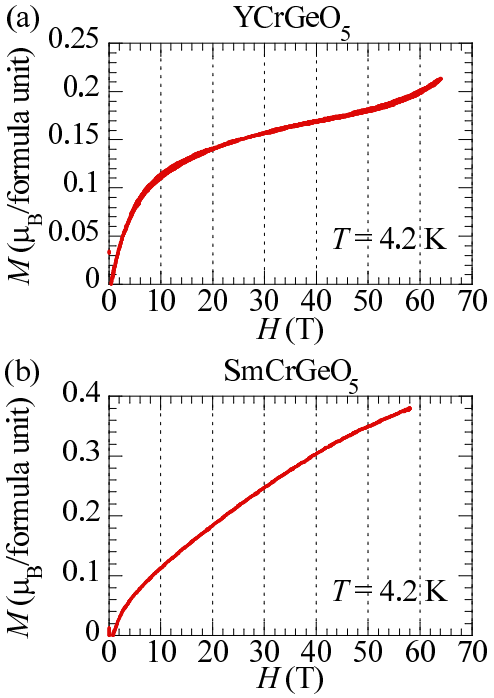

FIG. 4. (Color online) High-field magnetization at 4.2 K of $YCrGeO_5$ (a) and $SmCrGeO_5$ (b).

as 8.8%. Considering the $Y_2Ge_2O_7$ weight, we obtained the susceptibility in Fig. 3(a). The susceptibility of $YCrGeO_5$ at low T increases like a Curie-Weiss susceptibility probably because of unidentified magnetic material(s) in the $YCrGeO_5$ sample. We were unable to prove a spin-singlet GS with a spin gap because of the Curie-Weiss susceptibility. No magnetic transition appears down to 2 K. The susceptibility of our $SmCrGeO_5$ powders agrees with that reported by Shpanchenko *et al.* [26]. Results of analyses are described later.

We show high-field magnetizations at 4.2 K of $YCrGeO_5$ and $SmCrGeO_5$ powders in Figs. 4(a) and 4(b), respectively. An upturn of the magnetization of $YCrGeO_5$ is apparent around 55 T, suggesting spin-gap closing induced by the magnetic field. The spin-gap closing might occur in higher fields. The slope of the magnetization is small around $M = 0.15\ \mu_B$/formula unit, indicating that about 5% Cr^{3+} spins are nearly isolated. We did not observe an upturn in the magnetization of $SmCrGeO_5$ up to 58 T. The magnetization results suggest that $YCrGeO_5$ has a smaller spin gap than $SmCrGeO_5$. This point is consistent with INS results presented below.

We show INS results of $YCrGeO_5$ at 4.0 K and 199 K in Figs. 5(a) and 5(b), respectively, and those of $^{154}SmCrGeO_5$ at 7.8 K and 202 K in Figs. 6(a) and 6(b), respectively. The energies of incident neutrons E_i are 51.1 and 91.6 meV for the measurements of $YCrGeO_5$ and $^{154}SmCrGeO_5$, respectively. In $YCrGeO_5$, excitations are observed in the energy range of 8 meV $\lesssim \omega \lesssim$ 23 meV at 4.0 K and the intensity decreases with the increase of Q. The intensity of the excitations is suppressed at higher temperature, 199 K. The results mean that the observed excitations are dominated by those of magnetic origin. Furthermore, no excitation is observed at $\omega \lesssim 8$ meV and this means the existence of a spin gap. Qualitatively the same behaviors are observed in $^{154}SmCrGeO_5$. $YCrGeO_5$ and $^{154}SmCrGeO_5$ are the first spin-$\frac{3}{2}$ chain substances having a spin gap.

We obtained intensity maps in the k-ω plane as shown in Figs. 7(a) and 8(a) from the low-T data using the conversion method developed by Tomiyasu *et al.* [32]. The formula is given as follows:

$$S_{SX}^{(1D)}(Q_{1D},\omega) = \left[S_{pwd}(Q,\omega) + Q\frac{\partial S_{pwd}(Q,\omega)}{\partial Q} \right]_{Q=Q_{1D}}. \quad (2)$$

Here Q_{1D}, $S_{pwd}(Q,\omega)$, and $S_{SX}^{(1D)}(Q_{1D},\omega)$ represent the magnitude of the scattering vector parallel to the spin chain, the powder average scattering function, and the scattering function for Q_{1D} expected in a single crystal, respectively. The normalized wave number k is defined as $Q_{1D}\frac{d_1+d_2}{2}$. The values of $d_1 + d_2$ at room temperature are 5.68 and 5.72 Å for $YCrGeO_5$ and $SmCrGeO_5$, respectively [26]. The intensity is the strongest at around $k = \pi$, as expected in AF alternating spin chains. The magnetic excitations seem to have a dispersion relation. The white line in Figs. 7(a) and 8(a) shows the empirical dispersion relation of the lowest magnetic excitations $\omega(k) = \sqrt{A^2 \sin^2 k + \Delta^2}$. The values are $\Delta = 10$ meV and $A = 21$ meV in $YCrGeO_5$, and $\Delta = 18$ meV and $A = 15$ meV in $^{154}SmCrGeO_5$. Excitations seem to continue up to 29 meV around $k = 1.5\pi$ in Fig. 8(a). The empirical dispersion relation covering the energy range between 18 and 29 meV is not consistent with the positions of the excitations between 20 and 24 meV (not shown). We do not consider that

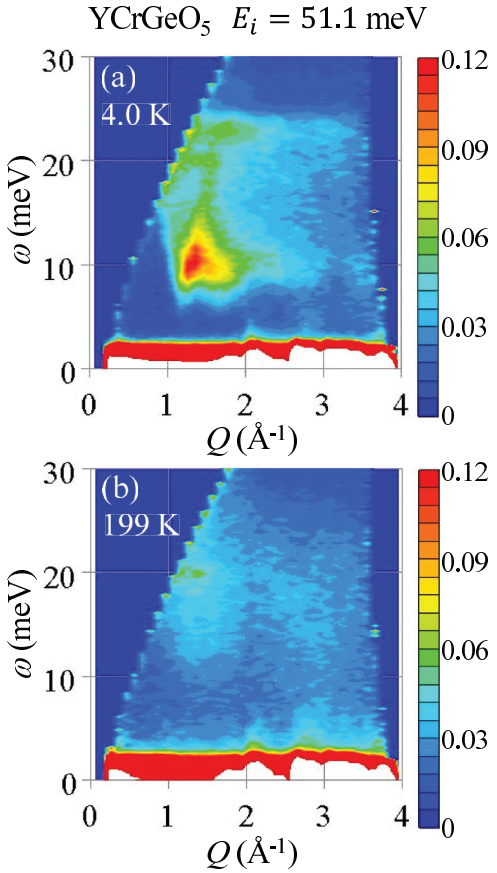

FIG. 5. (Color online) Maps of neutron scattering intensity in the Q-ω plane of $YCrGeO_5$ at 4.0 K (a) and 199 K (b). The energy of incident neutrons E_i is 51.1 meV. The numbers of protons injected to the neutron production target are about 1.47×10^{19} and 1.30×10^{19} for the measurements at 4.0 K and 199 K, respectively. When the beam power is 200 kW, the total number of protons per day is 3.6×10^{19}. The spent times are about 9.8 and 8.7 h for the measurements at 4.0 K and 199 K, respectively. The right vertical keys show the INS intensity in arbitrary units. The intensity is normalized to compare two data in different proton numbers.

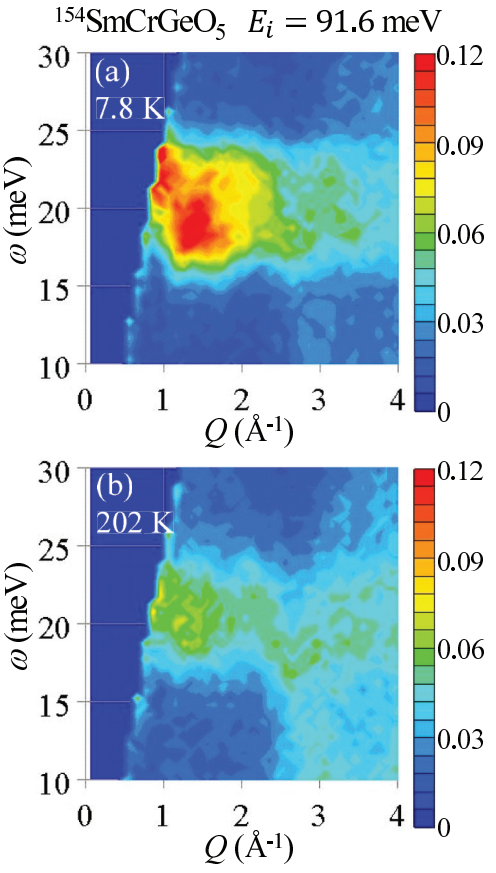

FIG. 6. (Color online) Maps of neutron scattering intensity in the Q-ω plane of $^{154}SmCrGeO_5$ at 7.8 K (a) and 202 K (b). The energy of incident neutrons E_i is 91.6 meV. The numbers of protons injected to the neutron production target are about 2.79×10^{19} and 2.60×10^{19} for the measurements at 7.8 K and 202 K, respectively. The spent times are about 18.6 and 17.3 h for the measurements at 7.8 K and 202 K, respectively. The right vertical keys show the INS intensity in arbitrary units. The intensity is normalized to compare two data in different proton numbers.

the excitations between 18 and 29 meV belong to one branch. The INS intensities around $Q = 1.65$ Å^{-1} ($k = 1.5\pi$) above 24 meV are small in Fig. 6(a). We are not confident that the excitations in the same ranges in Fig. 8(a) are intrinsic.

The origin of the spin gaps is the bond alternation of the nearest-neighbor (NN) exchange interactions and frustration between NN and next-nearest-neighbor (NNN) exchange interactions [33]. In AF Heisenberg uniform spin-$\frac{3}{2}$ chains with both NN and NNN exchange interactions (J_{NN} and J_{NNN}), the spin gap appears at $J_{NNN}/J_{NN} > 0.335$ [34]. Probably, the maximum value of Δ/J_{NN} is 0.2 or less [33,35]. Consequently, only the frustration between NN and NNN interactions cannot explain the observed large spin gaps.

We compare experimental INS intensities and calculated dynamical structure factors of the AF Heisenberg alternating spin-$\frac{3}{2}$ chains without NNN exchange interactions. The experimental values of $\omega(1.5\pi)/\omega(\pi)$ are 2.3 and 1.3 in $YCrGeO_5$ and $^{154}SmCrGeO_5$, respectively. When $\delta = 0.75$ and 0.90, values of $\omega(1.5\pi)/\omega(\pi)$ are 2.2 and 1.3 in the calculated results presented in Figs. 7(b) and 8(b), respectively. The calculated dynamical structure factors are similar to the experimental INS intensities. The intensity is asymmetric relative to $k = 1.5\pi$ in both experimental and calculated results. Both the results are qualitatively consistent with each other. In $YCrGeO_5$, however, excitations are hardly observed at $k > 1.5\pi$. Probably, it is difficult to observe clearly weak excitations in powder samples. In the calculated result with $\delta = 0.75$, $\Delta/J = 1.1$. Therefore, $J = 9.1$ meV $= 106$ K in $YCrGeO_5$. The ratio of the two exchange interaction values is $(1-\delta)/(1+\delta) = 0.14$. In the calculated result with $\delta = 0.90$, $\Delta/J = 1.6$. Therefore, $J = 11$ meV $= 128$ K in $^{154}SmCrGeO_5$. The value of $(1-\delta)/(1+\delta)$ is 0.05.

Figures 7(c) and 8(c) show constant Q spectra at $k = \pi$ of $YCrGeO_5$ at 4.0 K and $^{154}SmCrGeO_5$ at 7.8 K, respectively. A single peak is apparent around the gap energy in each line. We were unable to estimate accurately the energy resolution around 10 and 18 meV because of powder samples. The energy resolution around 10 and 18 meV is expected to be higher than that at 0 meV. Therefore, we compared the width of the peak

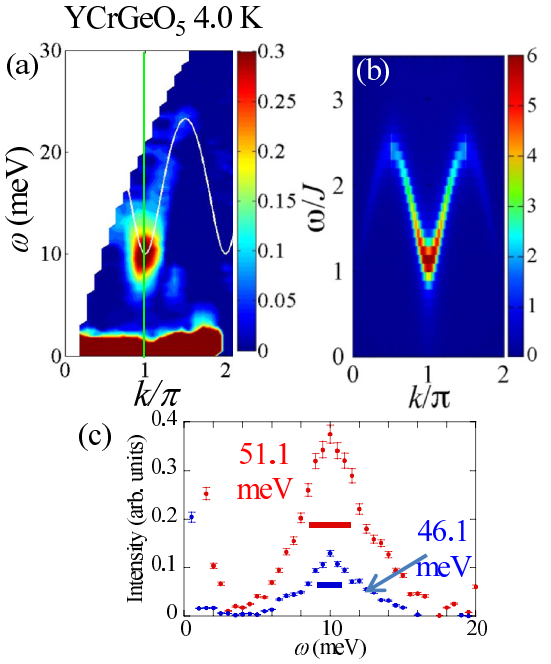

FIG. 7. (Color online) (a) Map of neutron scattering intensity in the k-ω plane of $YCrGeO_5$ at 4.0 K and $E_i = 51.1$ meV obtained using the conversion method [32]. The horizontal axis indicates the normalized wave number parallel to the spin chain. The right vertical key shows the INS intensity in arbitrary units. The white line indicates $\omega(k) = \sqrt{A^2 \sin^2 k + \Delta^2}$ with $\Delta = 10$ meV and $A = 21$ meV. (b) The dynamical structure factor of the AF Heisenberg alternating spin-$\frac{3}{2}$ chain with $\delta = 0.75$ calculated using the dynamical DMRG method. The right vertical key shows the intensity in arbitrary units. We used a Lorentzian broadening with half width at half maximum $\eta = 0.16J$. (c) Experimental constant-Q spectra at $k = \pi$ indicated by the green line in (a). Red and blue circles represent data at $E_i = 51.1$ and 46.1 meV (with a higher energy resolution), respectively. The horizontal bars represent the energy resolution at $\omega = 0$ meV.

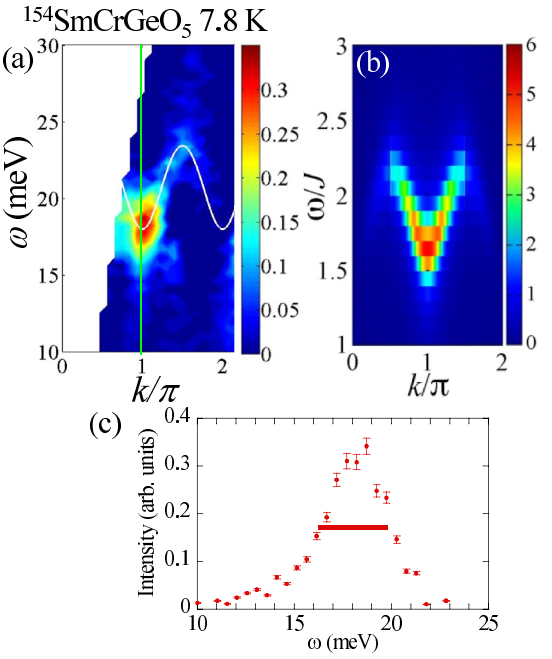

FIG. 8. (Color online) (a) Map of neutron scattering intensity in the k-ω plane of $^{154}SmCrGeO_5$ at 7.8 K and $E_i = 91.6$ meV obtained using the conversion method [32]. The horizontal axis indicates the normalized wave number parallel to the spin chain. The right vertical key shows the INS intensity in arbitrary units. The white line indicates $\omega(k) = \sqrt{A^2 \sin^2 k + \Delta^2}$ with $\Delta = 18$ meV and $A = 15$ meV. (b) The dynamical structure factor of the AF Heisenberg alternating spin-$\frac{3}{2}$ chain with $\delta = 0.9$ calculated using the dynamical DMRG method. The right vertical key shows the intensity in arbitrary units. We used a Lorentzian broadening with half width at half maximum $\eta = 0.16J$. (c) Experimental constant-Q spectrum (circles) at $k = \pi$ is indicated by the green line in (a). The horizontal bar represents the energy resolution at $\omega = 0$ meV.

with the energy resolution at 0 meV (horizontal bar). The width of the 10-meV peak in $YCrGeO_5$ is broader than the energy resolution. The 18-meV peak in $^{154}SmCrGeO_5$ is nearly resolution limited or might be slightly broader than the energy resolution. This result is consistent with the fact that the spin system of Cr^{3+} spins in $SmCrGeO_5$ $[(1-\delta)/(1+\delta) = 0.05]$ is similar to an isolated AF dimer.

We show in Fig. 3 that the experimental susceptibility is similar to the calculated one. The experimental χ_{exp} of $YCrGeO_5$ consists of three terms: χ_{Cr}, χ_{CW}, and χ_0. The first term χ_{Cr} is susceptibility of the alternating spin chain with $J = 106$ K and $\delta = 0.75$. The second term χ_{CW} is the Curie-Weiss term that is dominant at low T. In the two terms, we reasonably assume that the g value is 2 for Cr^{3+} spins. From the data below 10 K, we obtained $\chi_{CW} = \frac{0.052}{T-0.2}$ emu/mol, which means that about 2.8% of Cr spins are nearly isolated. Therefore, the green line of χ_{Cr} represents 0.972 of the molar susceptibility of the alternating spin chain. The third term χ_0 is a constant term. When $\chi_0 = -1.3 \times 10^{-4}$ emu/mol, the sum of the three terms χ_{cal} reproduces roughly the experimental χ_{exp}. We speculate that the negative value of χ_0 originates mainly in nonmagnetic $Y_2Ge_2O_7$. The sample used in the susceptibility measurement (2.8% isolated spins) differs from that used in the high-field magnetization measurement (5% isolated spins as aforementioned). We obtained a value close to 5% from the susceptibility of a sample took from the same batch used in the high-field magnetization measurement.

The experimental χ_{exp} of $SmCrGeO_5$ consists of three terms: χ_{Cr}, χ_{Sm}, and χ_0. The first term χ_{Cr} is susceptibility of the alternating spin chain with $J = 128$ K and $\delta = 0.9$. The second term χ_{Sm} is the Curie-Weiss term generated by Sm^{3+} ions. From the data below 30 K, we obtained $\chi_{Sm} = \frac{0.055}{T+0.22}$ emu/mol. The GS of Sm^{3+} ions is $^6H_{5/2}$, meaning that the value of $\boldsymbol{J}$ $(= \boldsymbol{L} + \boldsymbol{S})$ is $|L - S| = 5/2$. Here, $\boldsymbol{L}$ is the total angular momentum. The value of the Landé g factor is 2/7. Thus, the Curie constant of Sm^{3+} ions is calculated as 0.0893 emu K/mol, which is slightly larger than the experimental value. The third term χ_0 is a constant term. When $\chi_0 = 1.6 \times 10^{-3}$ emu/mol, the sum of the three terms χ_{cal} reproduces roughly the experimental χ_{exp}.

Figure 9 shows that the exchange interaction value decreases with the increasing Cr-Cr distance. Therefore, we consider that the $J(1+\delta)(\equiv J_1)$ and $J(1-\delta)(\equiv J_2)$ interactions exist in the d_2 and d_1 bonds, respectively, in Table I. The J_1 and J_2 values are 186 K and 26.5 K in $YCrGeO_5$ and

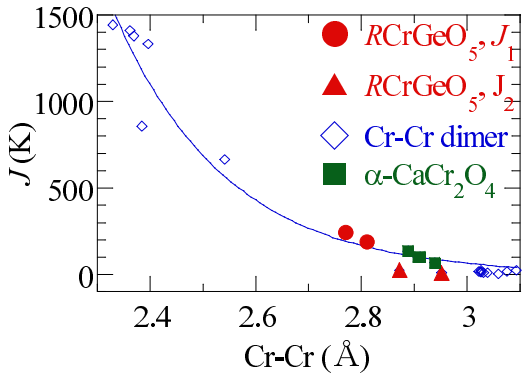

FIG. 9. (Color online) The exchange interaction value versus Cr-Cr distance. Circles and triangles represent the J_1 and J_2 values in RCrGeO$_5$ (R = Y or ^{154}Sm). Diamonds and squares represent the exchange interaction values in Cr-Cr dimer substances [36,37] and α-CaCr$_2$O$_4$ [38], respectively. The line indicates the empirical relation $J = a\exp(-R/b)$ with $a = 8.7 \times 10^7$ K and $b = 0.21$ Å [39].

243 K and 12.8 K in SmCrGeO$_5$. The d_2 and d_1 values are 2.811 and 2.872 Å in YCrGeO$_5$ and 2.770 and 2.952 Å in SmCrGeO$_5$. The J_1 values (circles) seem reasonable, whereas the J_2 values (triangles) are small as the Cr-Cr distances. We may underestimate the J_2 values. If we use J_1 and J_2 values expected from the line in Fig. 9, the calculated spin-gap values are smaller than the experimental values. Therefore, NNN exchange interactions must affect the spin-gap values. We consider that the main origin of the spin gaps is the bond alternation and that the spin-gap values are enlarged by the frustration between NN and NNN exchange interactions in the chains as in spin-$\frac{1}{2}$ chains [40]. Single-ion anisotropy may also affect the spin-gap values. The Cr atom is coordinated octahedrally by six oxygen atoms. Symmetries of crystal fields affecting the Cr^{3+} ions are nearly cubic. It is inferred that single-ion anisotropy of the Cr^{3+} ions is small. Therefore, we consider that influence of the single-ion anisotropy on the spin-gap value is small.

IV. CONCLUSION

We conducted INS and magnetization measurements on RCrGeO$_5$ (R = Y or Sm) powders. The high-field magnetization of YCrGeO$_5$ suggests the existence of a spin gap. We observed spin-gap (singlet-triplet) excitations and the dispersion relation of the lowest magnetic excitations in the INS results. The experimental results are consistent with the calculated results of the AF alternating spin-$\frac{3}{2}$ chain. YCrGeO$_5$ and SmCrGeO$_5$ are the first spin-$\frac{3}{2}$ chain substances having a spin-singlet GS with a spin gap. From the alternation ratio, the GS is expected to be the $(2S,0)$ state as shown in Fig. 1. Considering the small J_2 values as the Cr-Cr distances, we may overestimate the δ values. We consider that the main origin of the spin gaps is the bond alternation and that the spin-gap values are enlarged by the frustration between NN and NNN exchange interactions in the chains. We will study other RCrGeO$_5$. We expect to find substances of which GS is the $(2S-1,1)$ state as shown in Fig. 1.

ACKNOWLEDGMENTS

The neutron scattering experiments on ^{154}SmCrGeO$_5$ were approved by the Neutron Scattering Program Advisory Committee of IMSS, KEK (Proposal No. 2013S01). The neutron scattering experiments on YCrGeO$_5$ were approved by the Neutron Science Proposal Review Committee of J-PARC/MLF (Proposal No. 2012B0009) and supported by the Inter-University Research Program on Neutron Scattering of IMSS, KEK. The high-field magnetization experiments were conducted under the Visiting Researcher's Program of the Institute for Solid State Physics, the University of Tokyo. This work was supported by grants from NIMS. We are grateful to S. Matsumoto for sample syntheses and x-ray diffraction measurements, to M. Kaise for x-ray diffraction measurements, and to H. Sakurai for fruitful discussion. M.K. thanks S. Yamada and S. Nishimoto for helpful discussions on numerical techniques of the DMRG method. The theoretical work was supported by KAKENHI (No. 23540428) and the World Premier International Research Center Initiative (WPI), MEXT, Japan.

[1] Y. Kato and A. Tanaka, J. Phys. Soc. Jpn. **63**, 1277 (1994).
[2] M. Kohno, M. Takahashi, and M. Hagiwara, Phys. Rev. B **57**, 1046 (1998).
[3] M. Yajima and M. Takahashi, J. Phys. Soc. Jpn. **65**, 39 (1996).
[4] S. Yamamoto, Phys. Rev. B **55**, 3603 (1997).
[5] K. M. Diederix, H. W. J. Blöte, J. P. Groen, T. O. Klaassen, and N. J. Poulis, Phys. Rev. B **19**, 420 (1979).
[6] J. C. Bonner, S. A. Friedberg, H. Kobayashi, D. L. Meier, and H. W. J. Blöte, Phys. Rev. B **27**, 248 (1983).
[7] J. W. Bray, H. R. Hart, Jr., L. V. Interrante, I. S. Jacobs, J. S. Kasper, G. D. Watkins, S. H. Wee, and J. C. Bonner, Phys. Rev. Lett. **35**, 744 (1975).
[8] I. S. Jacobs, J. W. Bray, H. R. Hart, Jr., L. V. Interrante, J. S. Kasper, and G. D. Watkins, D. E. Prober, and J. C. Bonner, Phys. Rev. B **14**, 3036 (1976).
[9] M. Hase, I. Terasaki, and K. Uchinokura, Phys. Rev. Lett. **70**, 3651 (1993).
[10] M. Hase, I. Terasaki, Y. Sasago, K. Uchinokura, and H. Obara, Phys. Rev. Lett. **71**, 4059 (1993).
[11] M. Hase, I. Terasaki, K. Uchinokura, M. Tokunaga, N. Miura, and H. Obara, Phys. Rev. B **48**, 9616 (1993).
[12] Y. Narumi, M. Hagiwara, M. Kohno, and K. Kindo, Phys. Rev. Lett. **86**, 324 (2001).
[13] A. Zheludev, T. Masuda, B. Sales, D. Mandrus, T. Papenbrock, T. Barnes, and S. Park, Phys. Rev. B **69**, 144417 (2004).
[14] J. P. Renard, M. Verdaguer, L. P. Regnault, W. A. C. Erkelens, J. Rossat-Mignod, and W. G. Stirling, Europhys. Lett. **3**, 945 (1987).
[15] J. Darriet and L. P. Regnault, Solid State Commun. **86**, 409 (1993).
[16] J. F. DiTusa, S.-W. Cheong, C. Broholm, G. Aeppli, L. W. Rupp, Jr., and B. Batlogg, Physica B **194–196**, 181 (1994).
[17] T. Yokoo, T. Sakaguchi, K. Kakurai, and J. Akimitsu, J. Phys. Soc. Jpn. **64**, 3651 (1995).

[18] G. E. Granroth, M. W. Meisel, M. Chaparala, Th. Jolicoeur, B. H. Ward, and D. R. Talham, Phys. Rev. Lett. **77**, 1616 (1996).
[19] M. Hagiwara, Y. Idutsu, Z. Honda, and S. Yamamoto, J. Phys.: Conf. Ser. **400**, 032014 (2012).
[20] G. E. Granroth, S. E. Nagler, R. Coldea, R. S. Eccleston, B. H. Ward, D. R. Talham, and M. W. Meisel, Appl. Phys. A **74**, s868 (2002).
[21] O. Janson, S. Chen, A. A. Tsirlin, S. Hoffmann, J. Sichelschmidt, Q. Huang, Z.-J. Zhang, M.-B. Tang, J.-T. Zhao, R. Kniep, and H. Rosner, Phys. Rev. B **87**, 064417 (2013).
[22] K. Kakurai, M. Steiner, R. Pynn, and J. K. Kjems, J. Phys.: Condens. Matter **3**, 715 (1991).
[23] S. Itoh, T. Yokoo, S. Yano, D. Kawana, H. Tanaka, and Y. Endoh, J. Phys. Soc. Jpn. **81**, 084706 (2012).
[24] S. Itoh, Y. Endoh, K. Kakurai, H. Tanaka, S. M. Bennington, T. G. Perring, K. Ohoyama, M. J. Harris, K. Nakajima, and C. D. Frost, Phys. Rev. B **59**, 14406 (1999).
[25] S. Itoh, H. Tanaka, and M. J. Bull, J. Phys. Soc. Jpn. **71**, 1148 (2002).
[26] R. V. Shpanchenko, A. A. Tsirlin, E. S. Kondakova, E. V. Antipov, C. Bougerol, J. Hadermann, G. van Tendeloo, H. Sakurai, and E. Takayama-Muromachi, J. Solid State Chem. **181**, 2433 (2008).
[27] S. Itoh, T. Yokoo, S. Satoh, S. Yano, D. Kawana, J. Suzuki, and T. J. Sato, Nucl. Instrum. Methods Phys. Res., Sect. A **631**, 90 (2011).
[28] S. Yano, S. Itoh, T. Yokoo, S. Satoh, T. Yokoo, D. Kawana, and T. J. Sato, Nucl. Instrum. Methods Phys. Res., Sect. A **654**, 421 (2011).
[29] S. Itoh, K. Ueno, and T. Yokoo, Nucl. Instrum. Methods Phys. Res., Sect. A **661**, 58 (2012).
[30] H. G. Evertz, Adv. Phys. **52**, 1 (2003).
[31] E. Jeckelmann, Phys. Rev. B **66**, 045114 (2002).
[32] K. Tomiyasu, M. Fujita, A. I. Kolesnikov, R. I. Bewley, M. J. Bull, and S. M. Bennington, Appl. Phys. Lett. **94**, 092502 (2009).
[33] R. Roth and U. Schollwöck, Phys. Rev. B **58**, 9264 (1998).
[34] T. Hikihara, M. Kaburagi, and H. Kawamura, Phys. Rev. B **63**, 174430 (2001).
[35] F. Heidrich-Meisner, I. A. Sergienko, A. E. Feiguin, and E. R. Dagotto, Phys. Rev. B **75**, 064413 (2007).
[36] F. Albert Cotton, H. Chen, L. M. Daniels, and X. Feng, J. Am. Chem. Soc. **114**, 8980 (1992), and references therein.
[37] C. E. Talbot-Eeckelaers, G. Rajaraman, J. Cano, G. Aromi, E. Ruiz, and E. K. Brechin, Eur. J. Inorg. Chem. **2006**, 3382 (2006), and references therein.
[38] S. Toth, B. Lake, K. Hradil, T. Guidi, K. C. Rule, M. B. Stone, and A. T. M. N. Islam, Phys. Rev. Lett. **109**, 127203 (2012).
[39] M. Nishino, S. Yamanaka, Y. Yoshioka, and K. Yamaguchi, J. Phys. Chem. A **101**, 705 (1997).
[40] S. Watanabe and H. Yokoyama, J. Phys. Soc. Jpn. **68**, 2073 (1999).